Stability and structure changes of Na-titanate nanotubes at high temperature and high pressure

Huifang Xu,[1,a] Chenxiang Li,[1] Duanwei He,[2] and Yingbing Jinag[3]
[1]*Department of Geoscience, University of Wisconsin–Madison, Madison, Wisconsin 53706*
[2]*LANSCE, Los Alamos National Laboratory, Los Alamos, New Mexico 87545*
[3]*Department of Earth and Planetary Sciences, University of New Mexico, Albuquerque, New Mexico 87131*

(Received 7 March 2014; accepted 7 March 2014)

Stability of Na-titanate-based nanotubes at high temperature and pressure is investigated using X-ray diffraction and energy-dispersive X-ray diffraction (EDXRD). Our results show that the nanotubes can be stable at ~400 °C. Higher temperature annealing of nanotubes result in opening and flattening of the nanotubes, and subsequent structural transformation to $Na_2Ti_6O_{13}$-based structure via an intermediate phase with $Na_{0.23}TiO_2$-like structure. *In situ* EDXRD using diamond anvil cell indicates that the nanotubes collapse at about 15 GPa, and are finally transformed into an amorphous phase at about 30 GPa. The nanotubes kept in an amorphous state were further compressed to 50 GPa according to our *in situ* EDXRD observation. Titanate nanotubes are mechanically stronger than carbon nanotubes under static compression. © *2014 International Centre for Diffraction Data.*
[doi:10.1017/S0885715614000220]

Key words: Na-titanate, X-ray diffraction, energy-dispersive X-ray diffraction (EDXRD)

I. INTRODUCTION

Titanate-based nanotubes can be easily prepared using a hydrothermal synthesis method (Kasuga *et al.*, 1998; Tian *et al.*, 2003; Xu *et al.*, 2006). Owing to the high specific surface area, the nanotubes can be used as adsorbent (Bavykin *et al.*, 2005) and heterogeneous catalysts. The nanotube can be a potential photocatalyst because of its unique electrical polarity between inner- and outer surfaces (Xu *et al.*, 2006). Recent studies also show that nano-gold particles supported on titanate nanotubes and used as a heterogeneous catalyst may enhance low-temperature CO oxidation (Ntho *et al.*, 2008; Sikuvhihulu *et al.*, 2008; Mendez-Cruz *et al.*, 2011). It is important to understand the stability of the nanotubes at high temperature and high pressure in order to assure long-term performance of titanate nanotube-based materials. In this paper, we report systematic studies of the nanotubes at elevated temperatures and pressures.

II. SAMPLES AND EXPERIMENTAL METHODS

The Na-titanate nanotubes were prepared by adding 1 g of P25 powder to a 60 ml 10 M NaOH solution and annealing at 150 °C in digestion bomb for 20 h (Kasuga *et al.*, 1998; Xu *et al.*, 2006). The products were washed using distilled water until the water became neutral. Transmission electron microscope (TEM) analyses were carried out using a JEOL FEG-2010TEM with attached Oxford Instruments' X-ray energy-dispersive spectroscopy (EDS) system. In order to analyze thermal stability of the nanotubes, the synthesized Na-titanate nanotubes were annealed at different temperatures (400, 450, 500, and 800 °C) in air for different time periods. All X-ray diffraction (XRD) analyses of the nanotube samples and heated nanotube samples were carried out using a Rigaku Rapid II XRD system with a two-dimensional image plate (Mo$K\alpha$ radiation). The high pressure, *in situ* XRD experiments were carried out using a diamond anvil cell technique and energy-dispersive X-ray diffraction (EDXRD) at X-17C of NSLS of Brookhaven National Laboratory. We used bulk metallic glass as a gasket to avoid the interference of gasket XRD peaks with a samples' pattern.

III. RESULTS AND DISCUSSION

TEM images show that the sample is dominated by Na-titanate nanotubes that range from ~50 nm to several hundreds of nm (Figure 1). Diameters of nanotubes are very uniform. Inner diameters range from ~4 to ~5 nm. Outer diameters range from ~7 to ~10 nm. A high-resolution TEM image [Figure 1(B)] shows a smooth inner surface and some terraces on the outer surface. The structure of the nanotube matches that of $Na_2Ti_3O_7$ phase well, although X-ray energy-dispersive spectra show the Na/Ti ratio is lower than 2:3. The nanotubes or rolled sheets of the Na-titanate contain less Na with respect to flat and ideal $Na_2Ti_3O_7$. Results from Raman spectroscopy analyses show that nanotubes dried at 200 °C still contain OH in structure. It is proposed that H^+ may be incorporated into the structures of the nanotubes. The chemical formula for the H-bearing titanate nanotubes may be expressed as $(Na,H)_2Ti_3O_7$. A fast Fourier transform (FFT) pattern of the nanotube [Figure 2(B) insert] shows broad streaking (*h00* and *110*) reflections and a relatively sharp (*020*) reflection. The streaking is a result of the thin wall (only 3–5 repetitions) of the nanotube. The nanotube's elongation direction is ***b***-axis.

[a]Author to whom correspondence should be addressed. Electronic mail: hfxu@geology.wisc.edu

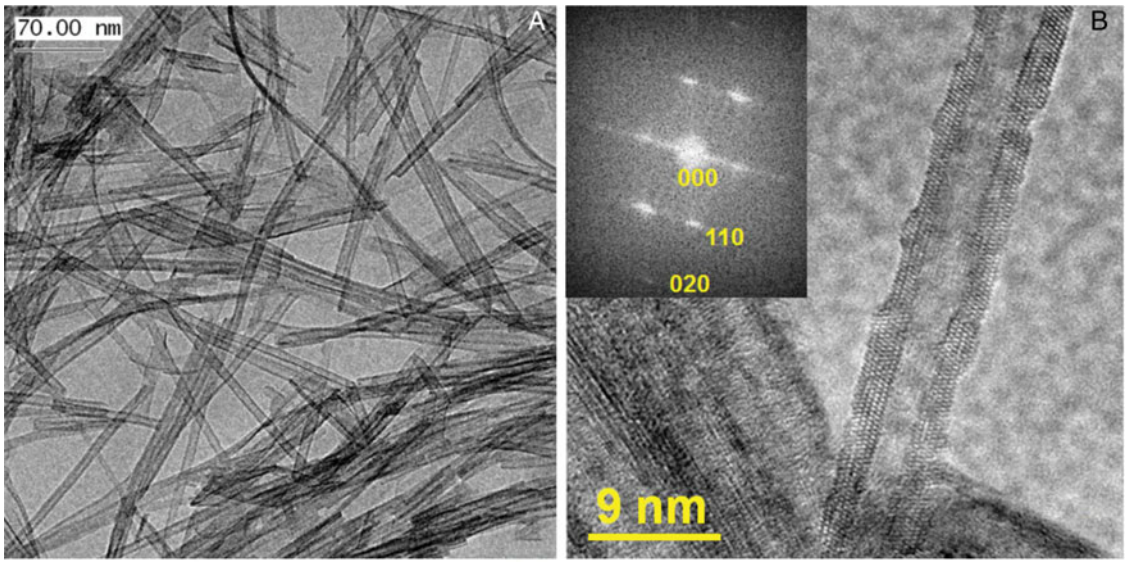

Figure 1. (Color online) (A) Bright-field TEM image showing Na-titanate nanotubes. (B) High-resolution TEM image showing a nanotube and its FFT pattern (insert at up-left corner). Indexing is based on a $Na_2Ti_3O_7$ phase with monoclinic symmetry although the number of Na for the nanotubes is less than 2 per formula, i.e. $(Na, H^+)_2Ti_3O_7$.

XRD patterns show that (001) peaks of $(Na, H)_2Ti_3O_7$ nanotubes are slightly shifted toward higher angle after the sample was annealed at 400, 450, and 500 °C for 1 h (Figure 1). Decreasing d_{001} spacing may be caused by dehydration of the nanotubes. At high temperature (e.g. 800 °C), the $(Na, H)_2Ti_3O_7$ nanotubes transformed into $Na_2Ti_6O_{13}$ completely within 1 h [Figure 2(E)]. Anatase appears as the sample is annealed for 8 h or longer at 800 °C [Figure 2(E)].

At low temperature (400 °C), the nanotubes are stable and show no change after the slight shift of the broad (001) diffraction peak. It is proposed that water molecules may be in the "interlayer-like" positions associated with H (Figure 3). Dehydration of interlayer-like water resulted in shrinking of d_{001} spacing from 9.91 to 8.54 Å. Rehydration of the dried sample resulted in expansion of d_{001} spacing from 8.54 to ~9 Å. Slight increase in d_{001} spacing indicates that the nanotubes were partially rehydrated (especially at the nanotube edges) at room temperature (Figure 3).

When the temperature is raised to 450 °C, the transformation begins after the sample has annealed for 16 h. An intermediate phase similar to the $Na_{0.23}TiO_2$ phase appears, although titanium has a valance state of +4 in the oxidizing environment. The intermediate phase appears even sooner at 500 °C [Figure 2(C)]. The final transformation product of $(Na,H)_2Ti_3O_7$ is $Na_2Ti_6O_{13}$. The intermediate phase similar to $Na_{0.23}TiO_2$ occurs at low temperature (Figure 2, B-16, B-32, C-8, and C-16 h) but not at high temperature [Figure 2(E)].

The structural evolution of $Na_2Ti_3O_7$ to $Na_2Ti_6O_{13}$ has been studied by Liu, H. *et al.* (2010). According to their paper, the synthesized $Na_2Ti_3O_7$ sample transformed into $Na_2Ti_6O_{13}$ when the crystals were annealed at 300 °C for 4 h under air. Their reported temperature is much lower than our observed transformation temperature. The nanotube structure may increase the stability of H-bearing Na-titanate $[(Na,H)_2Ti_3O_7]$. In their paper, the synthesized $Na_2Ti_3O_7$ product shows platy fibrous morphology and sharp peaks in the XRD pattern indicating the well-crystallized structure. If the intermediate product is ignored, the phase transformation of Na-titanate $[(Na,H)_2Ti_3O_7]$ nanotubes can be represented as follows:

$$2\,(Na,\ H)_2Ti_3O_7 \rightarrow Na_2Ti_6O_{13} + H_2O$$

The phase stability of the nanotubes at high pressure was also investigated using a diamond anvil cell technique and EDXRD at X-17C of NSLS. We used bulk metallic glass as a gasket to avoid the interference of gasket XRD peaks with a samples' pattern. In the EDXRD patterns, we focus on two peaks at ~2.3 Å (400 and $\bar{4}01$ diffraction peaks) and one peak at ~1.9 Å (020 diffraction peak) (Figure 4). The peak at ~1.9 Å is relatively sharp because the nanotube's elongation direction is ***b***-axis [Figures 1(A), 2(B) and 4). Intensity of the 1.9 Å peak decreases as the pressure increases (Figure 4). The peak disappears at ~29.5 GPa. Intensity of the 2.3 Å peak increases as the pressure increases to 15 GPa and higher (Figure 4), which indicates that the nanotubes collapse at about 15 GPa. Further increase in the pressure resulted in flatter nanotube and a stronger 400 diffraction peak. The nanotubes finally transformed into an amorphous phase at about 30 GPa. The nanotubes were kept in an amorphous state while further compressed to 50 GPa according to the XRD observation (Figure 4). It was reported that the microparticle and nanocrystalline anatase (TiO_2) started transforming to a baddeleyite structure at ~12–18 GPa. Additional Na may have kinetically hindered recrystallization of high-pressure TiO_2 phases after the nanotubes were crushed in our experiments.

Both single-wall carbon nanotubes and multi-wall carbon nanotubes collapse at pressure of ~10 GPa (Chesnokov *et al.*, 1999; Chen *et al.*, 2001; Venkateswaran *et al.*, 2001). The multi-wall carbon nanotubes were also reported to be in an amorphous state at 10–20 GPa by *in situ* XRD observation. The titanate nanotube is mechanically stronger than carbon nanotubes under static compression. Ionic bonding between neighboring Ti–O octahedral sheets through Na^+ is the major reason for the observed mechanical strength under static compression.

https://doi.org/10.1017/S0885715614000220 Published online by Cambridge University Press

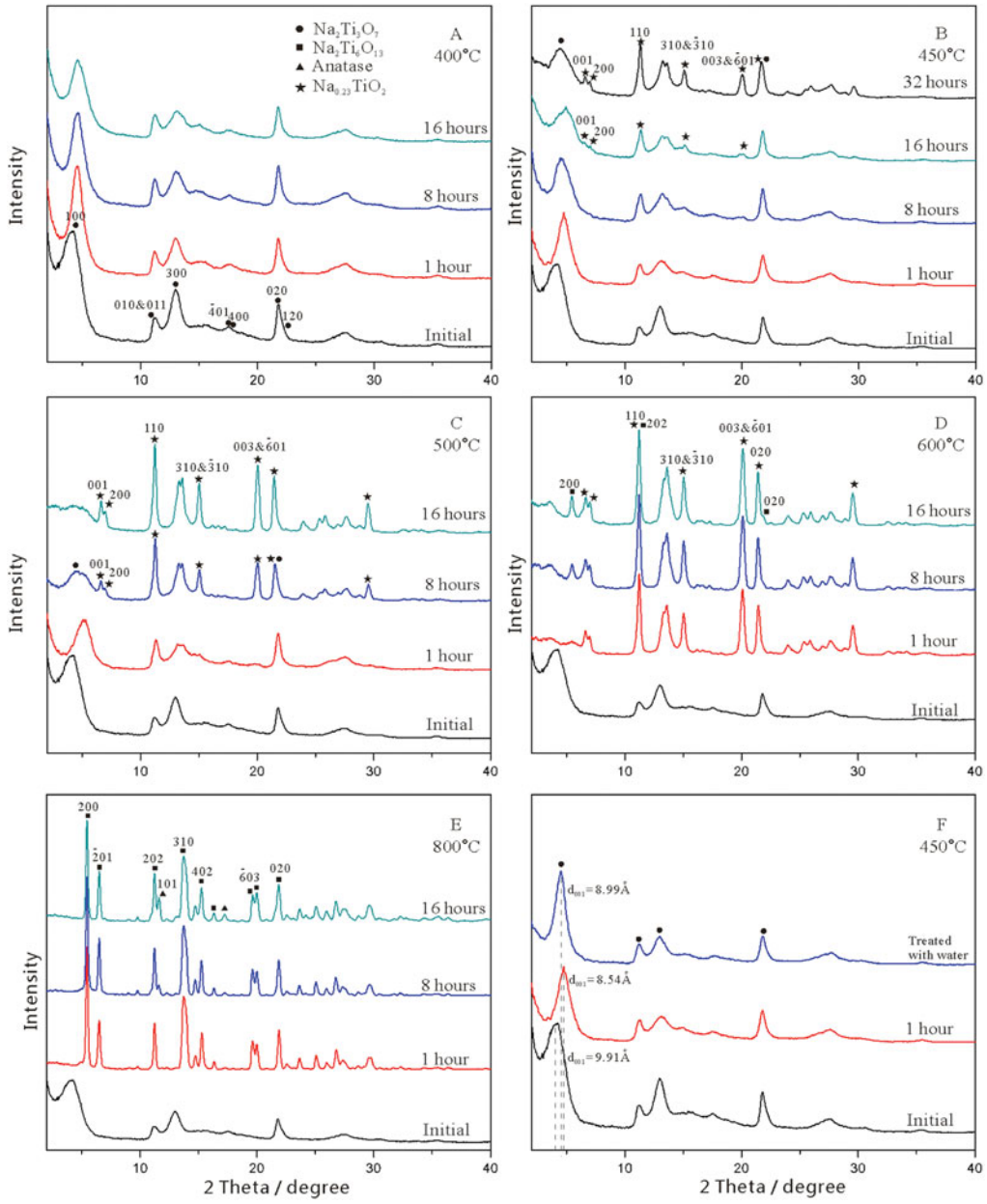

Figure 2. (Color online) XRD patterns of annealed products of the synthesized Na-titanate nanotubes at different temperatures for different times: (A) heated at 400 °C for 1, 8, and 16 h; (B) heated at 450 °C for 1, 8, 16, and 32 h; (C) heated at 500 °C for 1, 8, and 16 h; (D) heated at 600 °C for 1, 8, and 16 h; (E) heated at 800 °C for 1, 8, and 16 h; (F) heated at 450 °C for 1 h and then the product was soaked in water for 24 h at room temperature. "Initial" refers to the synthesized nanotubes at room temperature.

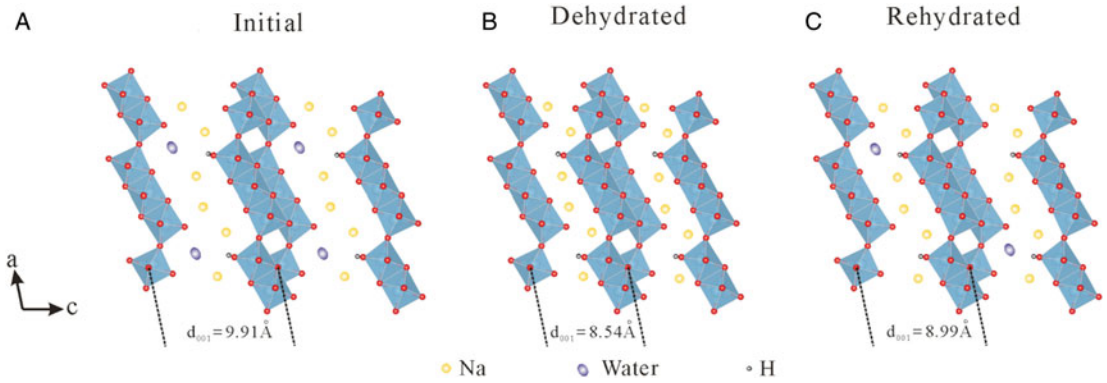

Figure 3. (Color online) Schematic diagram of the crystal structure change in synthesized nanotubes during the dehydration and rehydration processes. The amount of water in this diagram does not necessarily represent the stoichiometric ratio of water in the crystal structure. The (100) spacing difference is exaggerated in order to show differences among crystal structures.

https://doi.org/10.1017/S0885715614000220 Published online by Cambridge University Press

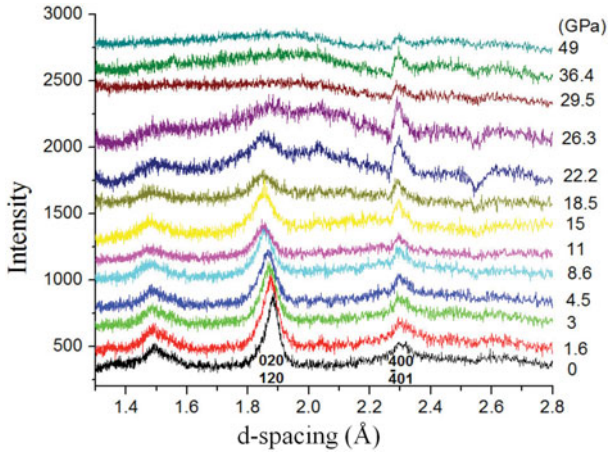

Figure 4. (Color online) *In situ* EDXRD patterns of the nanotubes under different pressures.

ACKNOWLEDGEMENTS

This work was supported by the NASA Astrobiology Institute (N07-5489). The authors acknowledge Brookhaven National Laboratory for using a beam line facility at NSLS. The authors also thank Mr. Nicholas Levitt for providing useful suggestions.

Bavykin, D., Lapkin, A., Plucinski, P., Friedrich, J., and Walsh, F. (**2005**). "Reversible storage of molecular hydrogen by sorption into multilayered TiO_2 nanotubes," J. Phys. Chem. B, **108**, 19422–19427.

Chen, L., Wang, L., Tang, D., Xie, S., and Jin, C. (**2001**). "X-ray diffraction study of carbon nanotubes under high pressure," Chin. Phys. Lett., **18**, 577–578.

Chesnokov, S. A., Nalimova, V. A., Rinzler, A. G., Smalley, R. E., and Fischer, J. E. (**1999**). "Mechanical energy storage in carbon nanotube springs," Phys. Rev. Lett., **82**, 343–346.

Kasuga, T., Hiramatsu, M., Hoson, A., Sekino, T., and Niihara, K. (**1998**). "Formation of titanium oxide nanotube," Langmuir, **14**, 3160–3163.

Liu, H., Yang, D., Zheng, Z., Ke, X., Waclawik, E., Zhu, H., and Frost, R. L. (**2010**). "A Raman spectroscopic and TEM study on the structural evolution of $Na_2Ti_3O_7$ during the transition to $Na_2Ti_6O_{13}$," J. Raman Spectrosc., **41**, 1331–1337.

Mendez-Cruz, M., Ramirez-Solis, J., and Zanella, R. (**2011**). "CO oxidation on gold nanoparticles supported over titanium oxide nanotubes," Catal. Today, **166**, 172–179.

Ntho, T. A., Anderson, J. A., and Scurrell, M. S. (**2008**). "CO oxidation over titanate nanotube supported Au: deactivation due to bicarbonate," J. Catalysis, **261**, 94–100.

Sikuvhihulu, L. C., Coville, N. J., Ntho, T. A., and Scurrell, M. S. (**2008**). "Potassium titanate: an alternative support for gold catalyzed carbon monoxide oxidation," Catal. Lett., **123**, 193–197.

Tian, Z. R., Voigt, J. A., Liu, J., Mckenzie, B., and Xu, H. (**2003**). "Large oriented arrays and continuous films of TiO2-based nanotubes," J. Am. Chem. Soc., **125**, 12384–12385.

Venkateswaran, U. D., Brandsen, E. A., Schlecht, U., Rao, A. M., Richter, E., Loa, I., Syassen, K., and Eklund, P. C. (**2001**). "High pressure studies of the Raman-active phonons in carbon nanotubes," Phys. Status Solidi b, **223**, 225–236.

Xu, H., Vanamu, G., Nie, Z., Konishi, H., Yeredla, R., Phillips, J., and Wang, Y. (**2006**). "Photocatalytic oxidation of a volatile organic component of acetaldehyde using titanium oxide nanotubes," J. Nanomater., **2006** (78902), 1–8.